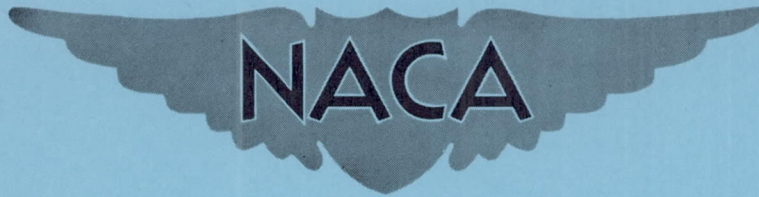


CONFIDENTIAL

Copy 249
RM L54K12a

NACA RM L54K12a



RESEARCH MEMORANDUM

EFFECTS OF BODY INDENTATION ON THE DRAG CHARACTERISTICS
OF A DELTA-WING—BODY COMBINATION AT TRANSONIC SPEEDS

By Dewey E. Wornom and Robert S. Osborne

Langley Aeronautical Laboratory
Langley Field, Va.

CLASSIFICATION CHANGED TO UNCLASSIFIED

AUTHORITY: NACA RESEARCH ABSTRACT NO. 121

EFFECTIVE DATE: OCTOBER 14, 1957 WHL

CLASSIFIED DOCUMENT

This material contains information affecting the National Defense of the United States within the meaning of the espionage laws, Title 18, U.S.C., Secs. 793 and 794, the transmission or revelation of which in any manner to an unauthorized person is prohibited by law.

**NATIONAL ADVISORY COMMITTEE
FOR AERONAUTICS**

WASHINGTON

January 28, 1955

CONFIDENTIAL

NATIONAL ADVISORY COMMITTEE FOR AERONAUTICS

RESEARCH MEMORANDUM

EFFECTS OF BODY INDENTATION ON THE DRAG CHARACTERISTICS
OF A DELTA-WING—BODY COMBINATION AT TRANSONIC SPEEDS

By Dewey E. Wornom and Robert S. Osborne

SUMMARY

Force tests of a delta-wing—body combination have been conducted in the Langley 8-foot transonic tunnel at Mach numbers from 0.60 to 1.14. Effects of body indentation based on the transonic area-rule concept for a Mach number of 1.0 were investigated at angles of attack up to approximately 10° . Additional tests were made to determine the transonic zero-lift drag characteristics of a delta-wing—body combination indented for a design Mach number of 1.4.

Body indentation for a Mach number of 1.0 resulted in transonic zero-lift drag-rise reductions of the order of 0.005 with little or no effect upon the lift and pitching-moment characteristics. The body indentation for a Mach number of 1.0 did not reduce the zero-lift drag rise of the wing-body combination to that of the basic body alone as would be expected from area-rule considerations.

The indentation for a Mach number of 1.4 revealed the same zero-lift drag reduction at Mach numbers up to 1.025 as that experienced by the indentation for a Mach number of 1.0. At higher Mach numbers, the drag reduction of the indentation for a Mach number of 1.4 was larger.

INTRODUCTION

The results of tests of delta-wing airplane configurations have indicated that these configurations had large zero-lift transonic drag rises. (See ref. 1, for example.) The high transonic drag was believed to be associated with the rather unfavorable axial distribution of total cross-sectional area.

In order to determine the extent to which the drag rise could be reduced by application of the transonic area-rule concept (ref. 2), a 60° delta wing having modified NACA 0004-65 airfoil sections was tested

in the Langley 8-foot transonic tunnel in combination with a body of revolution and in combination with the body of revolution indented for a design Mach number of 1.0 so that the cross-sectional area of the wing-body combination was the same as that for the basic body of revolution alone. In addition, the wing was tested with the body of revolution indented for a design Mach number of 1.4 (ref. 3) in order to determine the transonic-drag characteristics of a configuration designed for supersonic speeds. The results are presented herein.

The results of tests of the wing with the basic body of revolution and with the body indented for a Mach number of 1.0 in the Langley 4-foot supersonic pressure tunnel at Mach numbers of 1.41 and 2.01 are presented in reference 4.

SYMBOLS

M	free-stream Mach number
R	Reynolds number based on wing mean aerodynamic chord
α	angle of attack of wing chord line, deg
\bar{c}	wing mean aerodynamic chord, in.
S_B	model base area, sq ft
d	body diameter, in.
r	body radius, in.
x	longitudinal distance from nose, in.
S	total wing area including that blanketed by body, sq ft
L	lift, lb
D_B	base drag, $S_b(p_0 - p_b)$, lb
D	drag, Measured drag - Base drag, lb
M'	pitching moment about a point located at $0.275\bar{c}$ and $0.036\bar{c}$ above wing chord plane, in-lb
c	local chord, in.

C_L	lift coefficient, L/qS
C_m	pitching-moment coefficient, $\frac{M'}{qS\bar{c}}$
C_D	drag coefficient, D/qS
C_{D_0}	zero-lift drag coefficient
ΔC_D	incremental drag coefficient based on C_D value at $M = 0.60$
ΔC_{D_0}	incremental zero-lift drag coefficient based on C_{D_0} value at $M = 0.60$
$\partial C_m / \partial C_L$	static-longitudinal-stability parameter, averaged from $C_L = 0$ over linear portion of curve
$\partial C_L / \partial \alpha$	lift-curve slope per degree, averaged from $\alpha = 0^\circ$ over linear portion of curve
q	free-stream dynamic pressure, lb/sq ft
P_b	base-pressure coefficient, $\frac{P_b - P_o}{q}$
P_o	free-stream static pressure, lb/sq ft
p_b	static pressure at model base, lb/sq ft

APPARATUS AND METHODS

Tunnel

The investigation was conducted in the Langley 8-foot transonic tunnel which is a single-return system with a dodecagonal slotted test section. This test facility, operating at approximately atmospheric stagnation pressure, is capable of obtaining Mach numbers continuously through the speed of sound. Further details of the tunnel can be found in reference 5.

Models

The wing had 60° sweptback leading edges, 5° sweptforward trailing edges, and used modified NACA 0004-65 streamwise airfoil sections (table I). Other geometrical details of the wing, constructed of a steel leading edge and a tin bismuth surface formed over a steel core, are noted in figure 1. Chordwise fences were installed at the 66-percent-wing-semispan station and extended from the leading edge to the 79-percent-local-chord station. The fence height from the 10- to 50-percent-chord station was equal to the maximum local airfoil thickness. The fence was faired from the 10-percent-chord station to zero height at the leading edge, and from the 50-percent-chord station to a height of $1/8$ inch at the 79-percent-local-chord station. The fences were employed to alleviate adverse pitch-up tendencies which were found from previous tests to be characteristic of this wing.

The basic body of revolution was designed as a low wave drag body of given length, base diameter, and maximum diameter. An afterbody extension was used to reduce the base area to that of a typical interceptor fuselage (figs. 1 and 2).

The body indented for a Mach number of 1.0 was designed in accordance with the transonic area-rule concept so that the cross-sectional area of the wing-body combination at a given longitudinal station was the same as that of the basic body alone. The body indented for a Mach number of 1.4 was designed in accordance with reference 3. This design is the application of the supersonic area-rule concept in which the wing area removed from the body cross-sectional area is that average area cut by planes tangent to the design Mach cone at various roll angles. It should be noted that the slight increase in length of the body indented for $M = 1.4$ as compared with the other bodies tested has no special significance and was due to an inadvertent error in construction. Area distributions of the wing-body combinations are presented in figure 3 and body ordinates are listed in table II. Body fineness ratios are presented in table III.

Support System

The models were securely fastened to an internal strain-gage balance which was in turn attached to a support sting. At its downstream end, the sting was fastened through a 5° offset coupling to a support tube which was fixed axially in the center of the tunnel by two sets of support struts coming from the tunnel wall.

Measurements and Accuracies

Lift, drag, and pitching-moment measurements were obtained by the use of an internal electrical strain-gage balance. The pitching moment was measured about a point located at 27.5 percent of the mean aerodynamic chord and 3.6 percent of the mean aerodynamic chord above the chord plane.

The accuracy of the coefficients was estimated to be within the following maximum values up to a lift coefficient of at least 0.4:

C_L	± 0.005
C_D	± 0.001
C_m	± 0.001

The angle of attack was set using a fixed-pendulum strain-gage unit located in the support sting and an optical measuring device outside of the tunnel test section and is believed to be accurate within $\pm 0.15^\circ$. Support-system deflections were corrected by a calibration of sting and balance deflection with respect to model load.

Base pressures were obtained by an orifice located inside the base of the body. The accuracy of the base-pressure coefficients presented was estimated to be within ± 0.005 .

The average test Mach number was determined to within ± 0.003 from a calibration with respect to the pressure in the chamber surrounding the slotted test section.

Tests

The wing plus basic body and the wing plus body indented for $M = 1.0$ were tested at Mach numbers from 0.60 to 1.14 through an angle-of-attack range from 0° to approximately 10° . The wing plus body indented for $M = 1.4$ and the basic body alone were tested at Mach numbers from 0.60 to 1.14 for zero angle of attack only.

The test Reynolds number based on the wing mean aerodynamic chord was of the order of 4.4×10^6 (fig. 4).

Corrections

Boundary interference at subsonic velocities has been minimized by the slotted test section and no corrections have been applied. At Mach numbers above 1.00, the effects of boundary-reflected disturbances are

considered insignificant with the possible exception of a Mach number of 1.075. At a Mach number of 1.14, the disturbances had passed downstream of the model base.

Sting interference effects on lift and pitching-moment coefficients were probably negligible (ref. 6). The effect on drag was alleviated by adjusting the base pressure to free-stream conditions.

RESULTS

All data have been adjusted to represent free-stream static pressure at the model base using the base-pressure coefficients presented in figure 5.

Basic force and moment data for the wing plus basic body, wing plus body indented for $M = 1.0$, wing plus body indented for $M = 1.4$, and basic body alone are presented in figures 6 to 8. Body alone data have been based upon wing area. Analysis of figures 9 to 11 shows the effect of the transonic ($M = 1.0$) and supersonic ($M = 1.4$) indentations on the lift, drag, and pitching-moment characteristics.

Schlieren photographs of the four configurations tested are shown in figures 12 and 13.

DISCUSSION

Inasmuch as the variation of subsonic drag level due to body indentation indicated in figures 9 and 10(a) is unexplained on the basis of existing experimental results, it has been assumed for the present analysis that they would not exist on a full-scale airplane. Accordingly, in addition to the presentation of basic data, the drag variations with Mach number are presented as increments of pressure drag between that at any Mach number and a Mach number of 0.60. It should be pointed out that the incremental reduction in drag so obtained is conservative; that is, the reductions in drag resulting from any specific modification should be at least as large as those presented.

Indentation for $M = 1.0$

Zero-lift drag.- The Mach number 1.0 indentation reduced the zero-lift drag-rise coefficient by 0.005 at a Mach number of 1.0, and by values decreasing to 0.0007 at a Mach number of 1.14 (fig. 9). Some effects of indentation in reducing the strength of the shock waves at transonic speeds are indicated in the schlieren photographs of figures 12 and 13.

The zero-lift drag-rises of the wing plus body indented for $M = 1.0$ and basic body alone should be approximately equal on the basis of the area-rule concept since both configurations have the same cross-sectional area distribution. It was indicated in figure 9, however, that the peak drag-rise value of the wing plus body indented for $M = 1.0$ is 0.0122 or 61 percent higher than the 0.0076 value for the basic body alone. The difference is probably due to severe local velocity gradients created by the severe body indentations as stated in reference 7. The effects of the adverse velocity gradients are clearly shown by the shock formations of the wing plus body indented for $M = 1.0$ in figure 12(c) as compared with those of the basic body alone in figure 12(a).

Drag at lifting conditions.- Figure 10(b) presents a comparison of incremental drag (between any Mach number and a Mach number of 0.60) at lifting conditions between the wing plus basic body and wing plus body indented for $M = 1.0$. For $C_L = 0.2$ indentation resulted in a reduction in drag coefficient from $M = 0.95$ to 1.075 with a maximum reduction of 0.004 occurring near $M = 1.0$. For $C_L = 0.4$ indentation resulted in a reduction in drag coefficient from $M = 0.925$ to the highest test Mach number with the maximum reduction of 0.006 occurring at a Mach number of approximately 1.0.

Lift and pitching moment.- The lift-curve slope in figure 11 shows a slight increase of not more than 5 percent at Mach numbers above 0.9 as a result of indenting the basic body. No significant change in pitching-moment characteristics due to body indentation is noted. (See figs. 6(c) and 11.)

Indentation for $M = 1.4$

Drag at zero lift.- Zero-lift drag coefficient of the wing plus body indented for $M = 1.4$ was approximately equal to that of the wing plus body indented for $M = 1.0$ up to a Mach number of 1.025 (fig. 9). From Mach numbers of 1.025 to 1.14, the supersonic indented configuration zero-lift drag coefficient was approximately 0.002 lower than that of the transonic indented configuration.

Due to the limited angle of view and two-dimensional aspects of the schlieren photographs in figure 13, a comparison between the transonic and supersonic indented configurations at Mach numbers of 1.075 and 1.14 does not reveal the complete shock phenomenon. From the schlieren photographs, it appears that the transonic indented configuration resulted in less severe shocks than did the supersonic indented configuration. However, this may be misleading. Since the supersonic area rule is based upon reduction of shock formation in every plane that can be passed

through the longitudinal axis of the configuration, schlieren photographs at various angles of rotation about the longitudinal axis of the model, particularly a plan view where the disturbances of the wing would probably be more pronounced, would be more representative of the complete shock phenomenon.

CONCLUSIONS

The following may be concluded from wind-tunnel tests of a delta-wing--body combination with body indentations based on the transonic and supersonic area rule concept:

1. Body indentation for a Mach number of 1.0 resulted in transonic zero-lift drag-rise coefficient reductions of the order of 0.005.

2. The body indentation for $M = 1.0$ did not reduce the zero-lift drag rise of the wing-body combination to that of the basic body alone as would be expected from area-rule considerations.

3. Body indentation based on the transonic-area-rule concept had little or no effect upon the lift and pitching-moment characteristics.

4. The indentation for a Mach number of 1.4 revealed the same zero-lift drag reduction at Mach numbers up to 1.025 as that experienced by the indentation for a Mach number of 1.0. At higher Mach numbers the drag reduction of the $M = 1.4$ indentation was larger.

Langley Aeronautical Laboratory,
National Advisory Committee for Aeronautics,
Langley Field, Va., October 28, 1954.

REFERENCES

1. Bellman, Donald R., and Sisk, Thomas R.: Preliminary Drag Measurements of the Consolidated Vultee XF-92A Delta-Wing Airplane in Flight Tests to a Mach Number of 1.01. NACA RM L53J23, 1954.
2. Whitcomb, Richard T.: A Study of the Zero-Lift Drag-Rise Characteristics of Wing-Body Combinations Near the Speed of Sound. NACA RM L52H08, 1952.
3. Whitcomb, Richard T., and Fischetti, Thomas L.: Development of a Supersonic Area Rule and an Application to the Design of a Wing-Body Combination Having High Lift-to-Drag Ratios. NACA RM L53H31a, 1953.
4. Carlson, Harry W.: Preliminary Investigation of the Effects of Body Contouring As Specified by the Transonic Area Rule on the Aerodynamic Characteristics of a Delta Wing-Body Combination at Mach Numbers of 1.41 and 2.01. NACA RM L53G03, 1953.
5. Ritchie, Virgil S., and Pearson, Albin O.: Calibration of the Slotted Test Section of the Langley 8-Foot Transonic Tunnel and Preliminary Experimental Investigation of Boundary-Reflected Disturbances. NACA RM L51K14, 1952.
6. Osborne, Robert S.: High-Speed Wind-Tunnel Investigation of the Longitudinal Stability and Control Characteristics of a 1/16-Scale Model of the D-558-2 Research Airplane at High Subsonic Mach Numbers and at a Mach Number of 1.2. NACA RM L9C04, 1949.
7. Whitcomb, Richard T.: Recent Results Pertaining to the Application of the "Area Rule." NACA RM L53I15a, 1953.

TABLE I

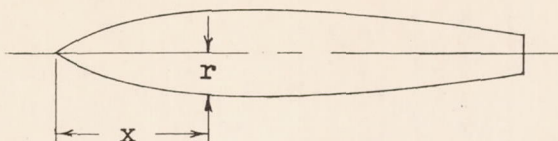
ORDINATES OF THE NACA 0004-65 (MODIFIED)

AIRFOIL SECTION

Station, percent c	Ordinate, percent c
0	0
.25	.28
.50	.39
.75	.47
1.00	.53
1.25	.59
2.50	.79
5.00	1.03
7.50	1.20
10.00	1.32
20.00	1.64
30.00	1.83
40.00	1.95
50.00	2.00
60.00	1.97
70.00	1.82
80.00	1.40
90.00	.73
100.00	----
Leading-edge radius: 0.0018c	

TABLE II

BODY ORDINATES



Model station, x, in. from nose	r for basic body, in.	r for indented body (M = 1.0), in.	r for indented body (M = 1.4), in.
0	0	0	0
.378	.162	.162	.162
1.512	.453	.453	.453
3.025	.749	.749	.749
6.050	1.220	1.220	1.220
9.075	1.590	1.590	1.590
12.100	1.890	1.880	1.890
13.000	-----	-----	1.950
15.000	-----	-----	2.020
15.130	2.110	2.000	-----
17.000	-----	-----	2.040
18.150	2.240	1.990	-----
19.000	-----	-----	2.010
21.000	-----	-----	1.870
21.180	2.200	1.800	-----
23.000	-----	-----	1.720
24.200	2.020	1.580	-----
25.000	-----	-----	1.650
27.000	-----	-----	1.590
27.230	1.840	1.650	-----
28.690	-----	1.770	-----
29.000	-----	-----	1.510
30.250	1.680	1.680	-----
31.000	-----	-----	1.440
33.370	1.260	1.260	-----
33.870	-----	-----	1.330

TABLE III

BODY FINENESS RATIOS

Configuration	Body length, in.	Maximum body diameter, in.	Body fineness ratio	Equivalent fineness ratio
Basic body alone	33.37	4.48	7.45	7.45
Wing plus body	33.37	4.48	7.45	6.57
Wing plus body indented for $M = 1.0$	33.37	4.00	8.34	7.45
Wing plus body indented for $M = 1.4$	33.87	4.08	8.31	7.42

CONFIDENTIAL

CONFIDENTIAL

NACA RM L54K12a

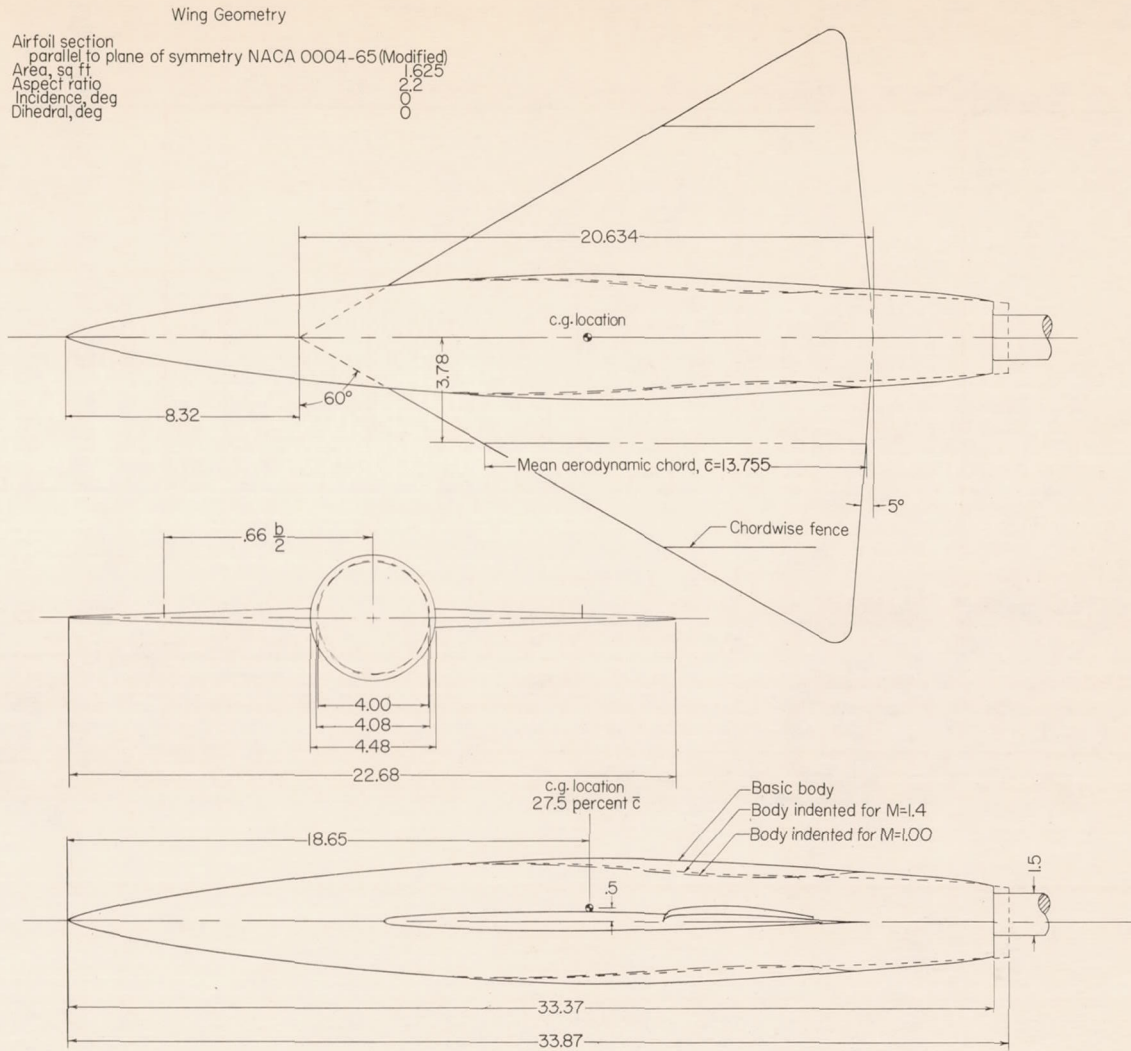
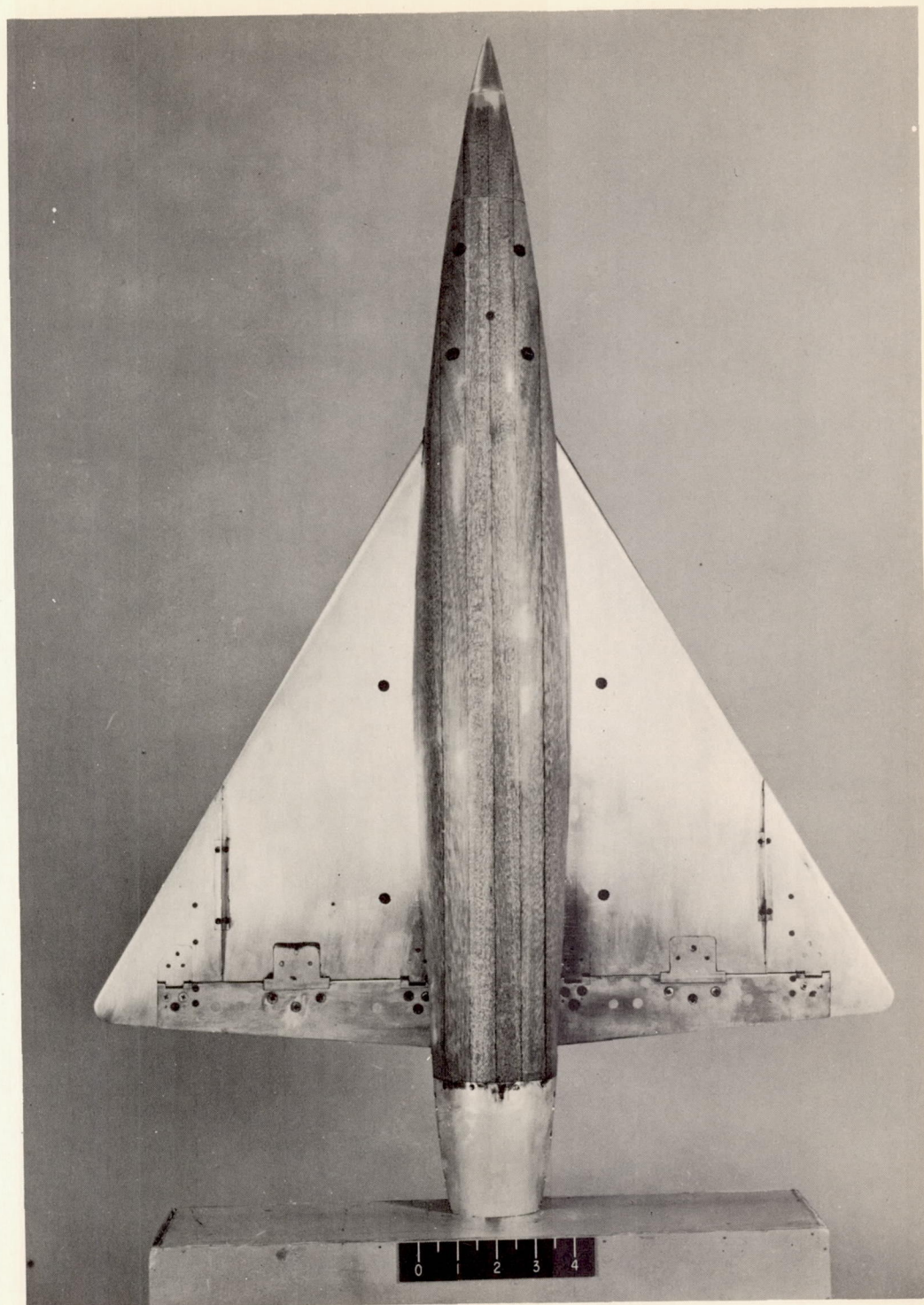


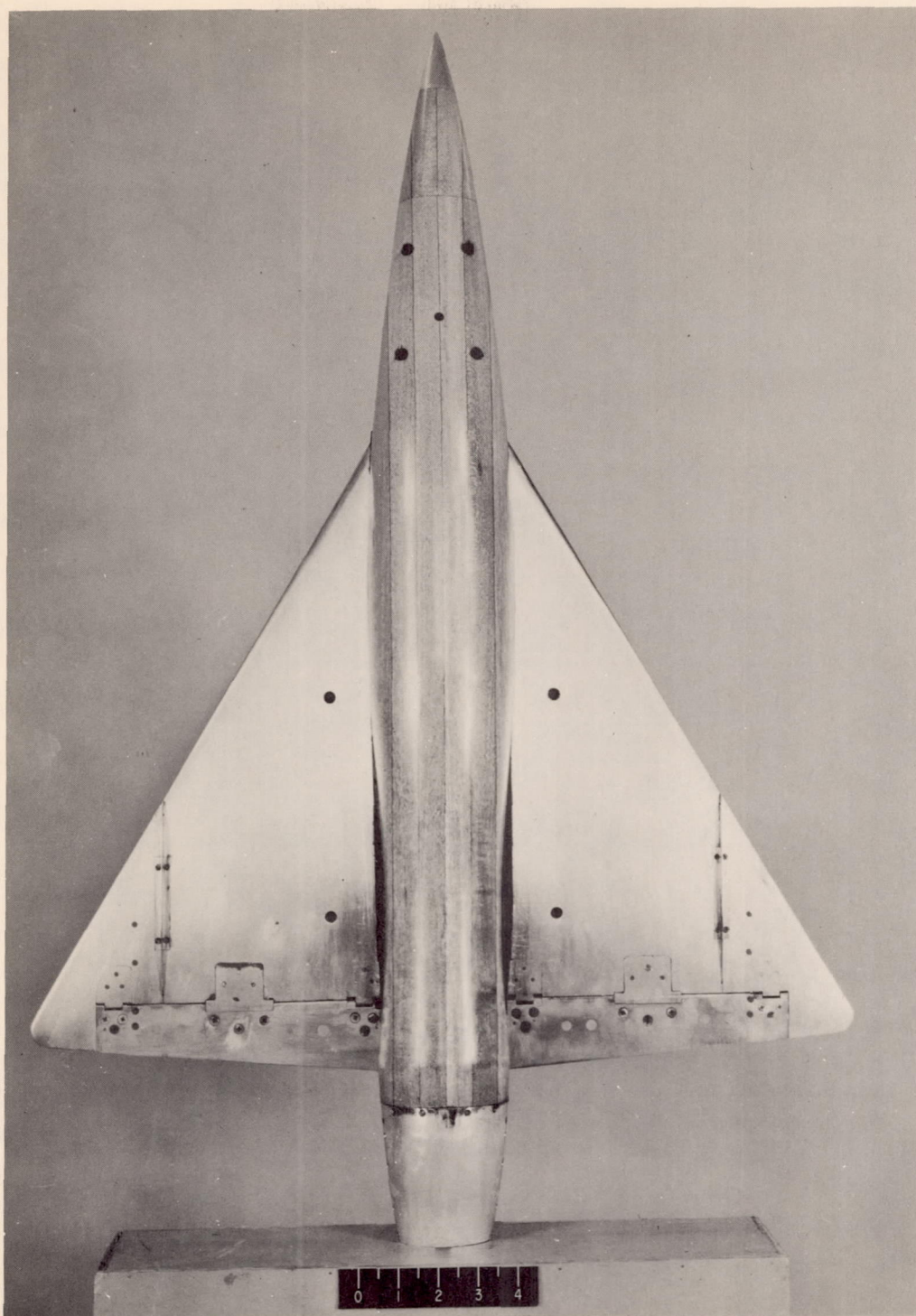
Figure 1.- Details of the wing-body combinations. All dimensions in inches unless otherwise noted.



(a) Wing plus body (basic).

L-78323.1

Figure 2.- Photographs of two configurations tested.



(b) Wing plus body indented for $M = 1.0$.

L-78324.1

Figure 2.- Concluded.

- Wing plus body (basic)
- - - Wing plus body indented for M=1.0
- Wing plus body indented for M=1.4
- - - Wing alone

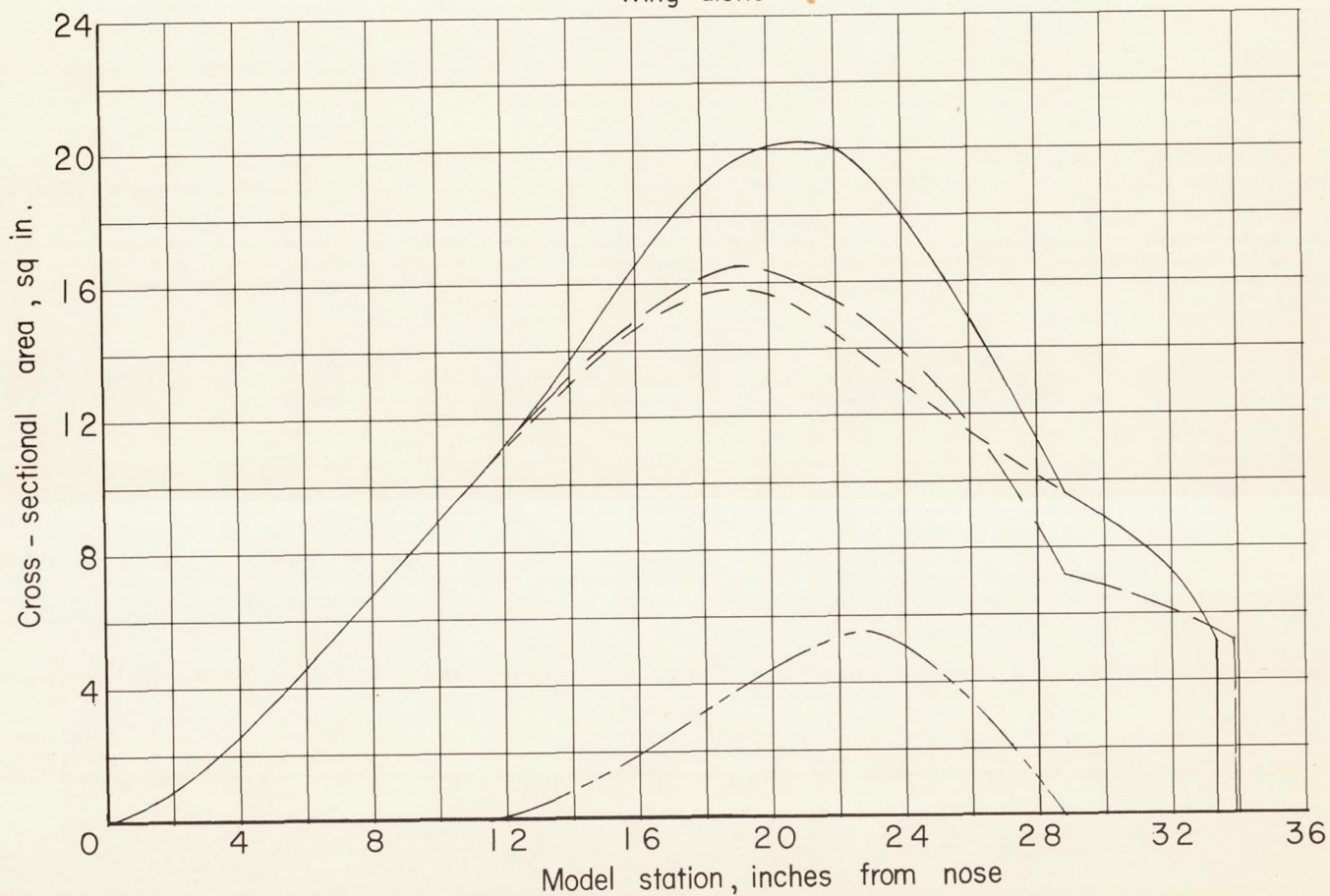


Figure 3.- Cross-sectional areas normal to the longitudinal body axis for the wing-body combinations.

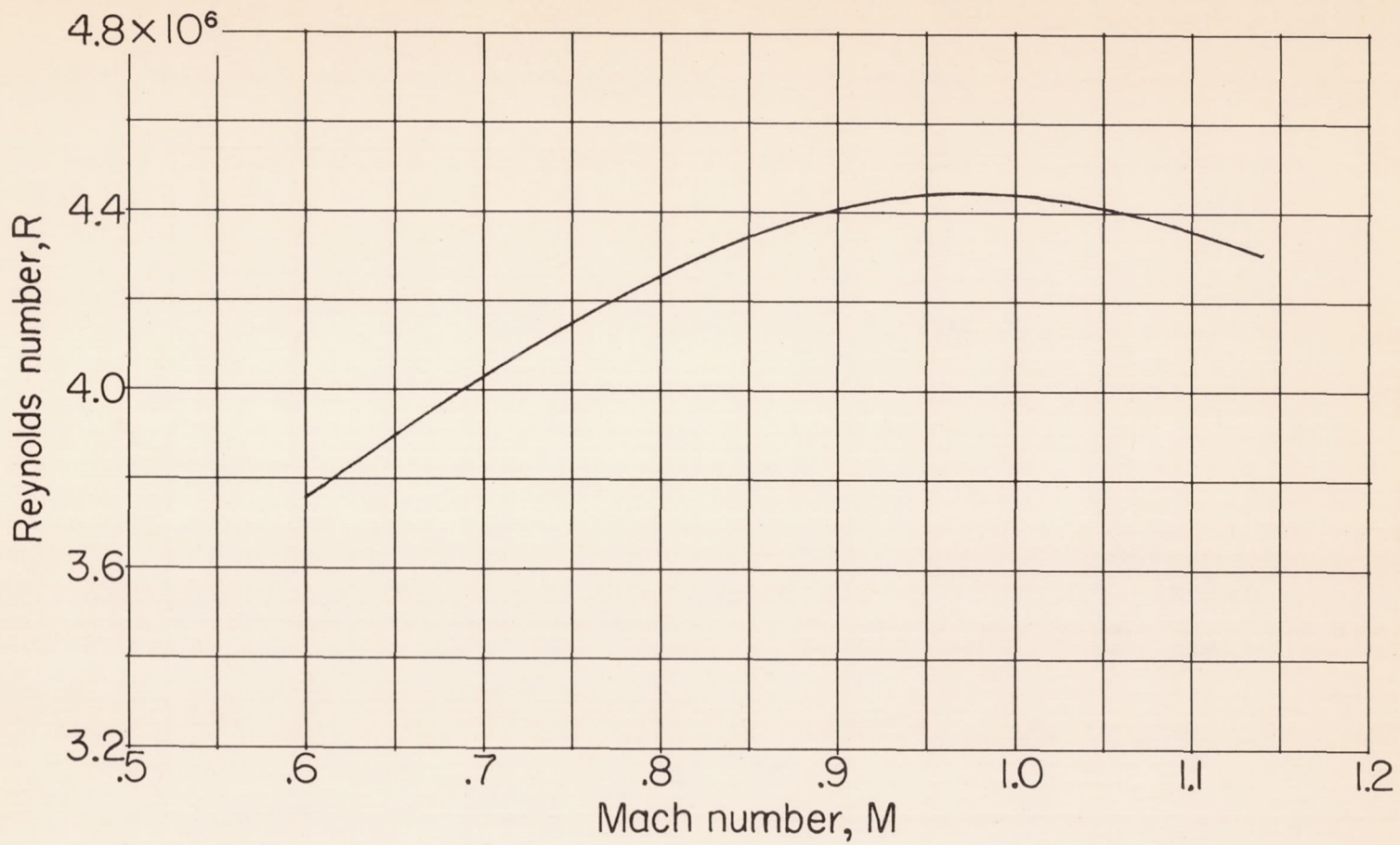


Figure 4.- Variation with Mach number of approximate test Reynolds number based on $\bar{c} = 13.755$ inches.

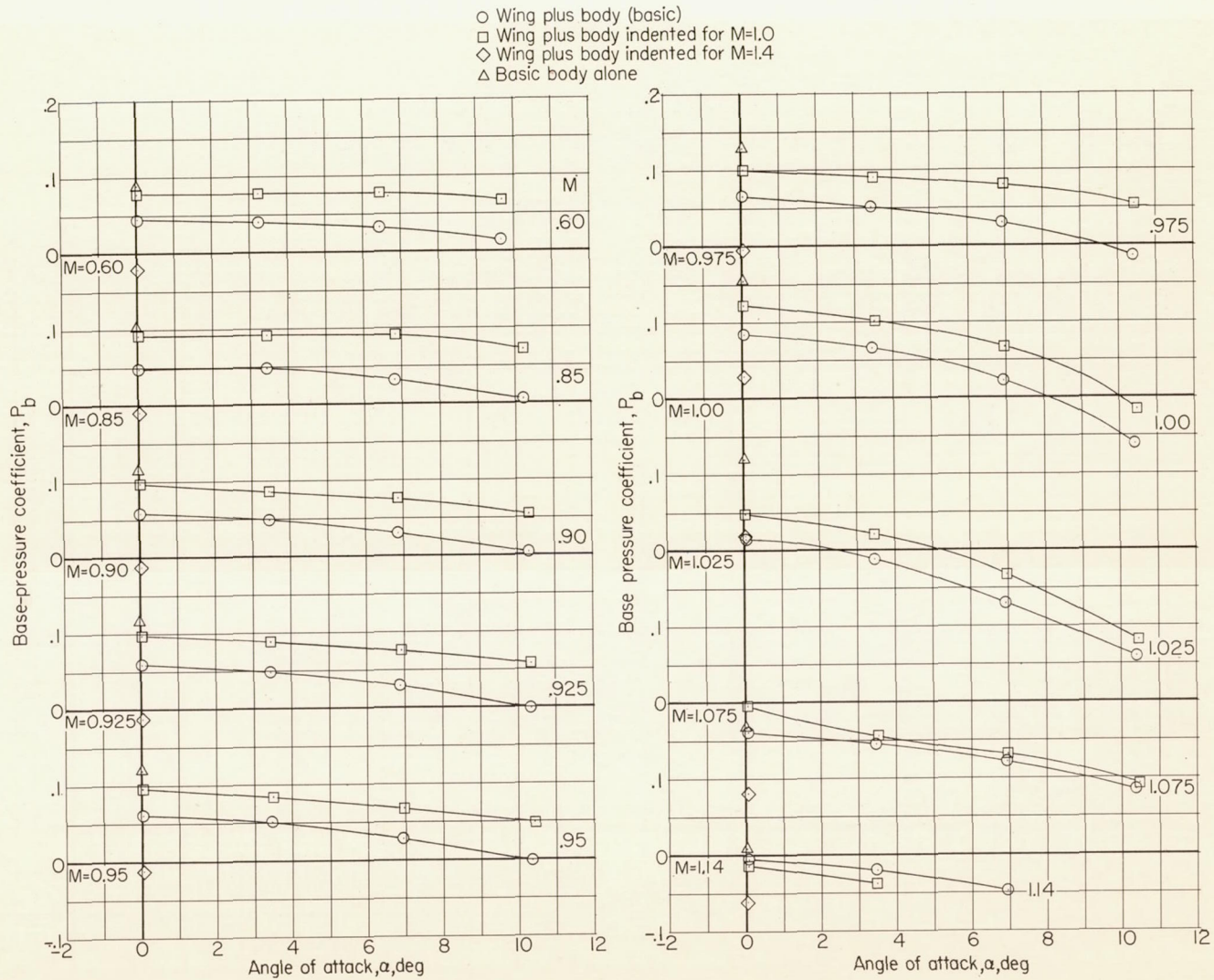
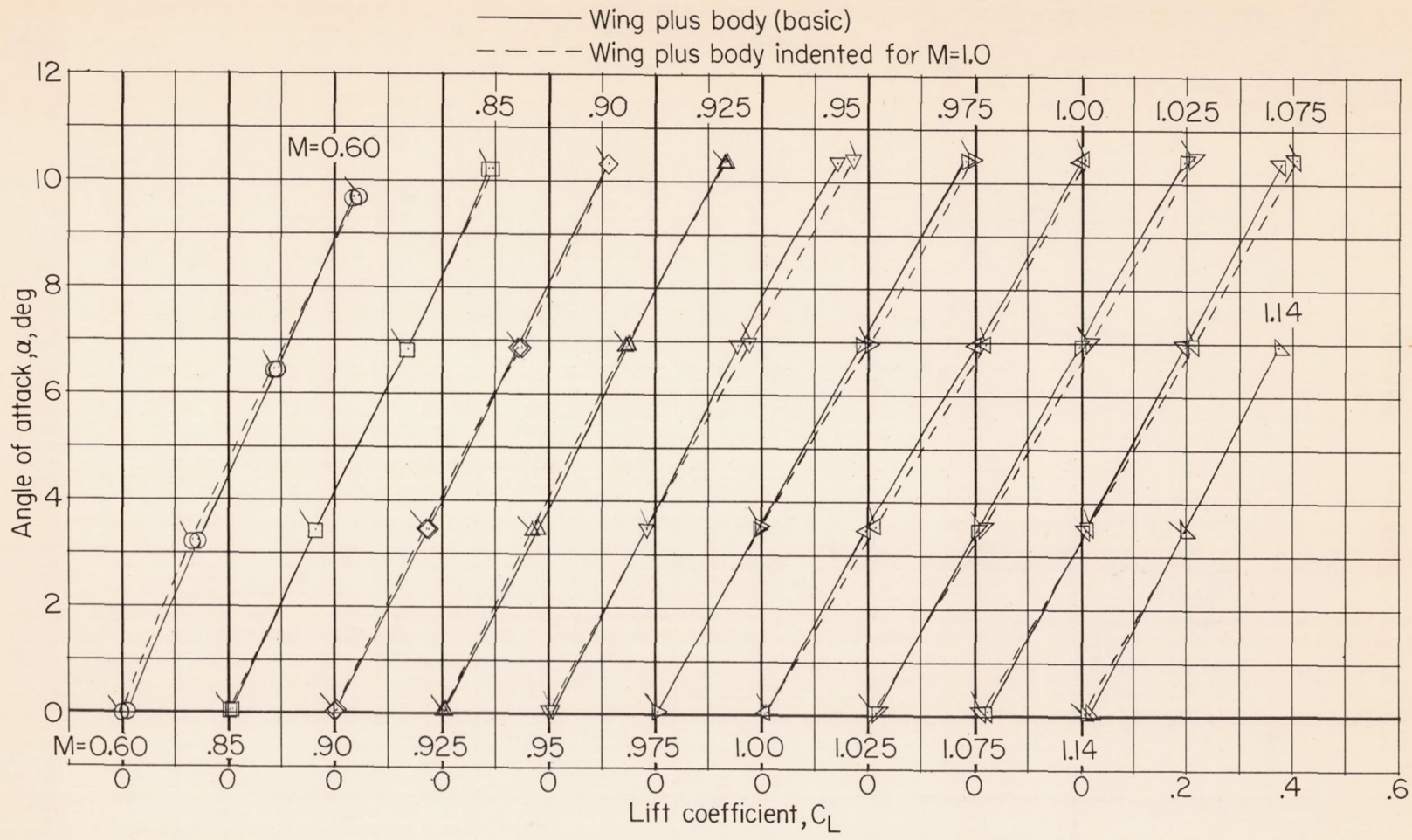


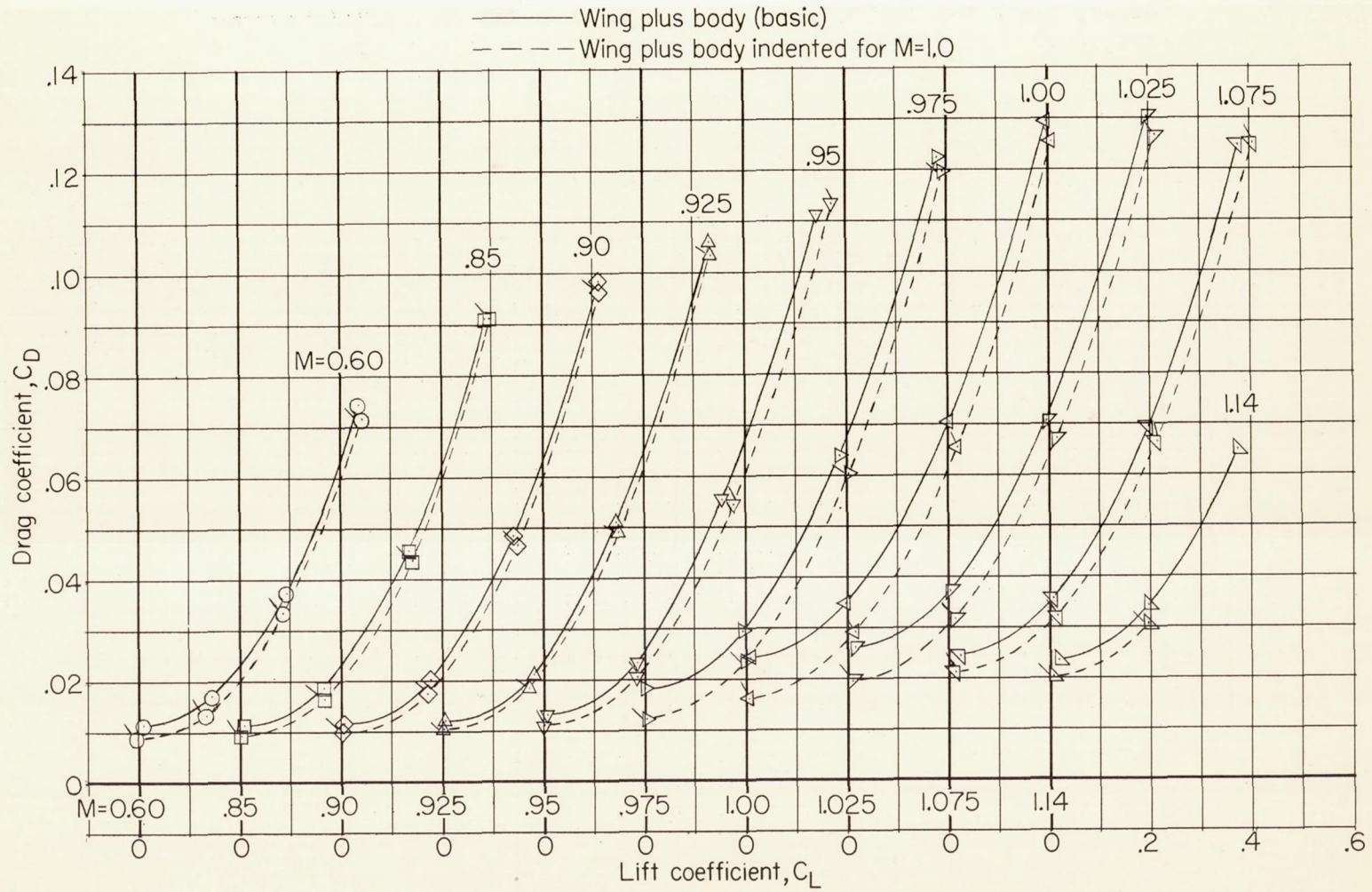
Figure 5.- Base-pressure coefficients for configurations tested.



(a) Lift.

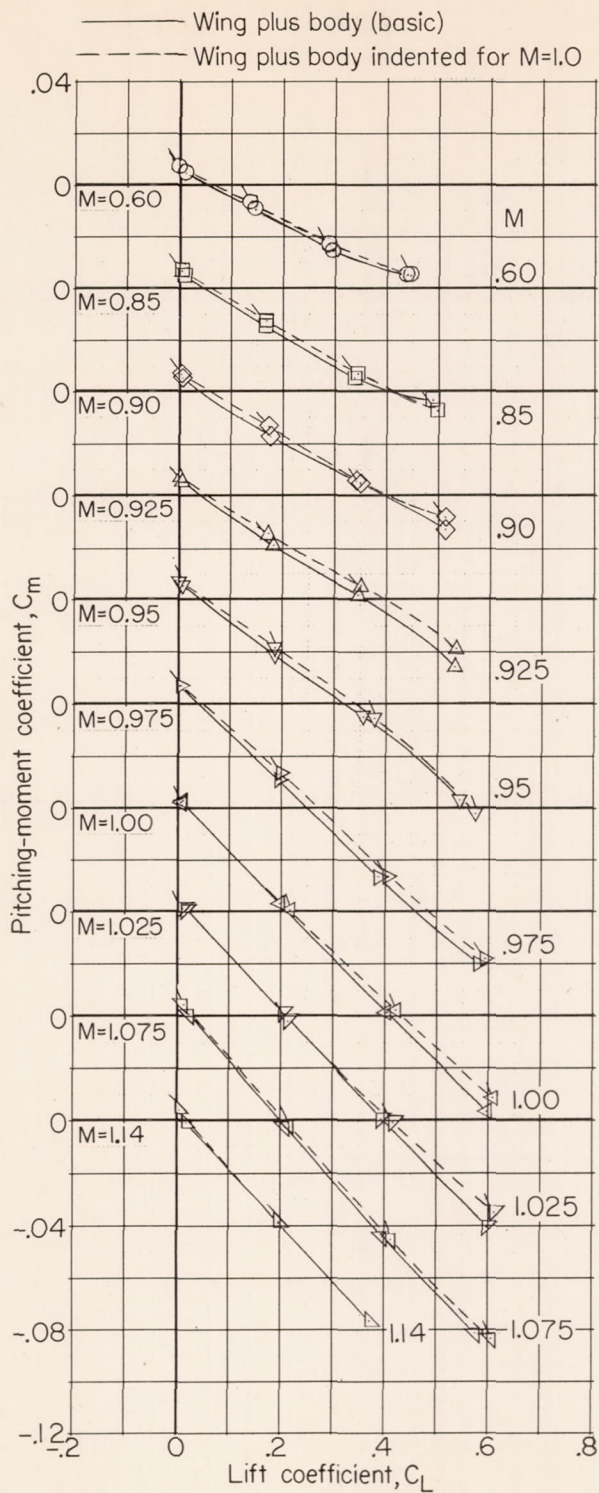
Figure 6.- Force and moment characteristics of the wing plus body (basic) and wing plus body indented for M = 1.0. Flagged symbols indicate M = 1.0 body.

CONFIDENTIAL



(b) Drag.

Figure 6.- Continued.



(c) Pitching moment.

Figure 6.- Concluded.

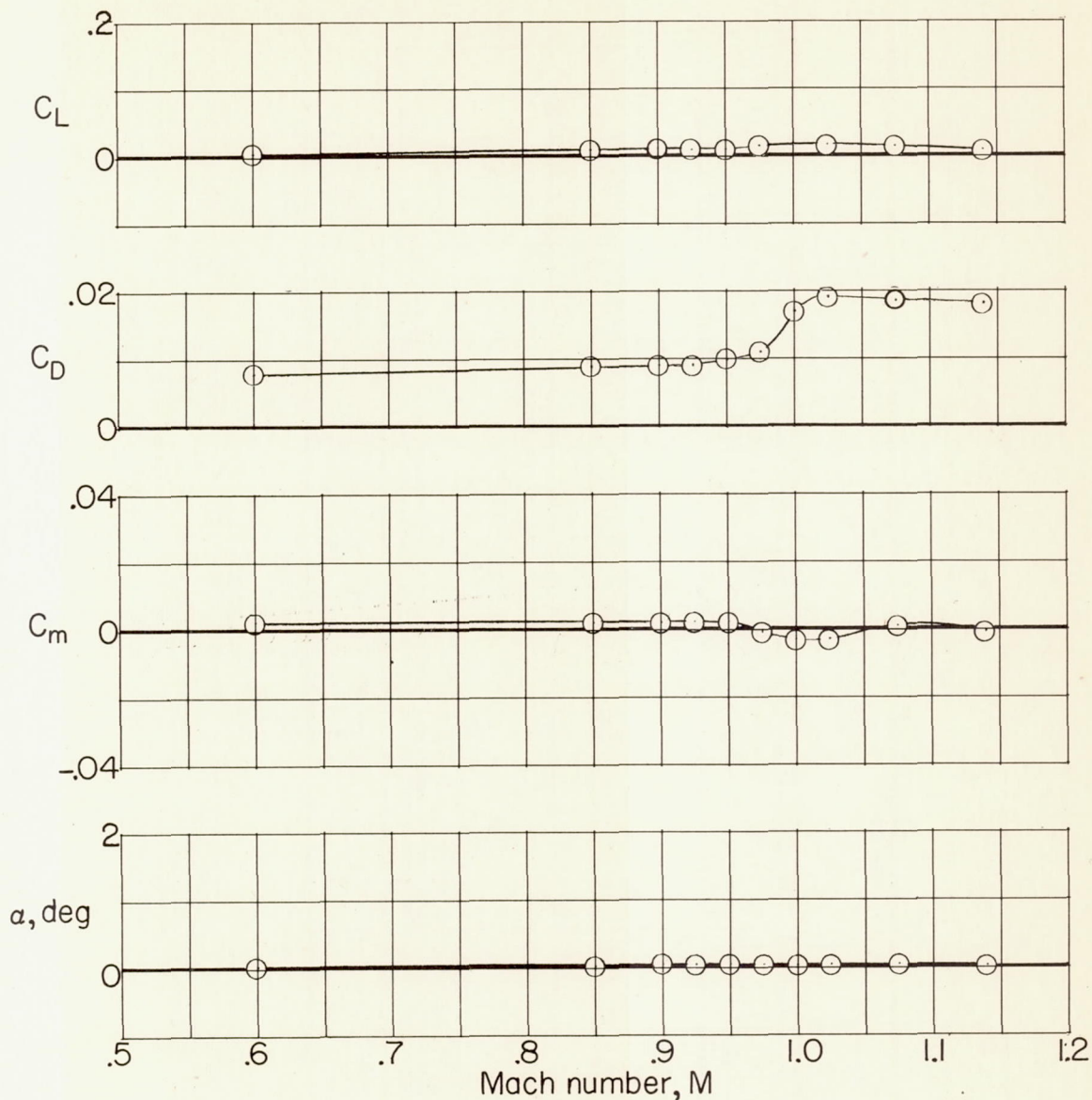


Figure 7.- Force and moment characteristics of the wing plus body indented for $M = 1.4$.

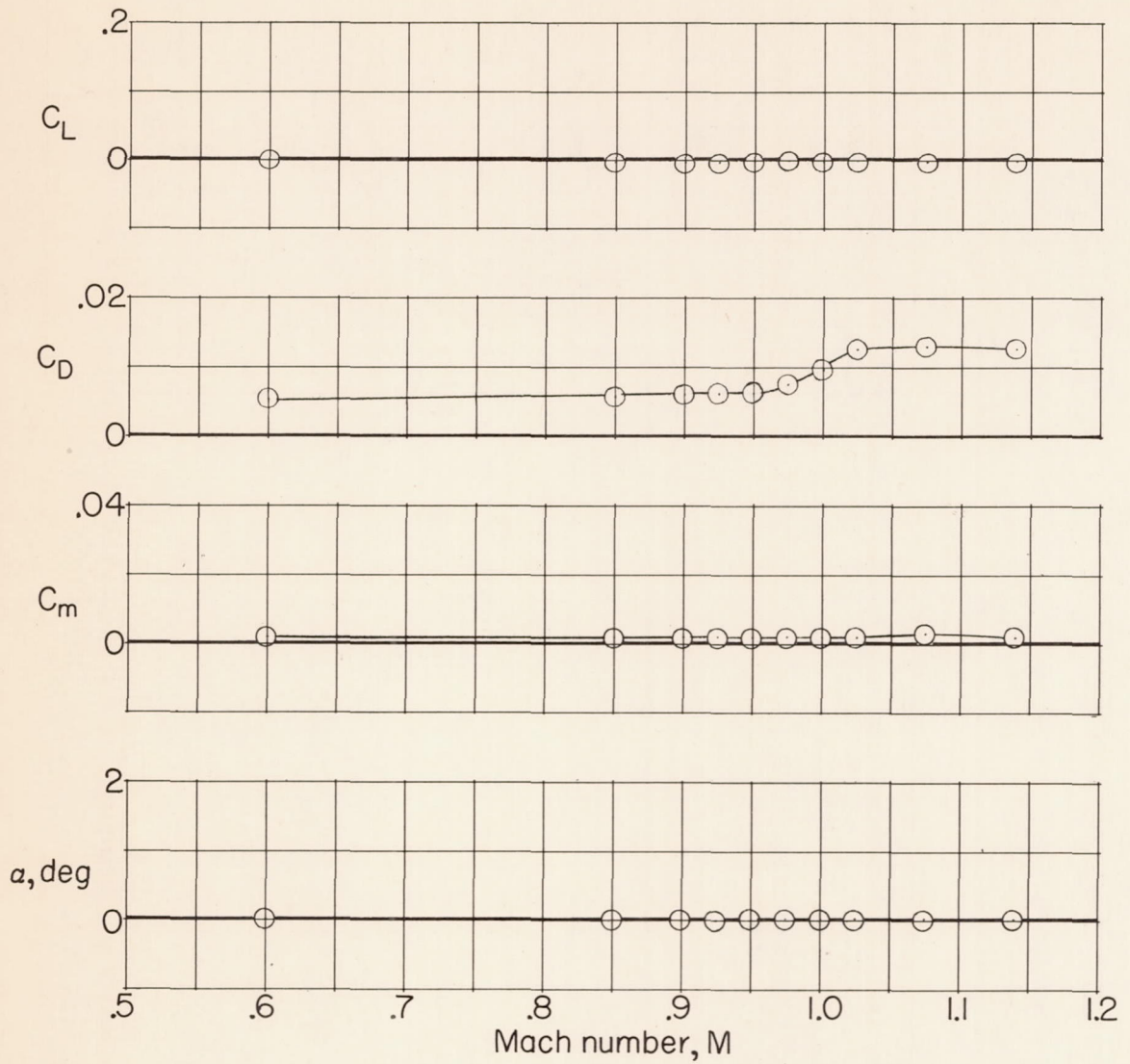


Figure 8.- Force and moment characteristics of the basic body alone.

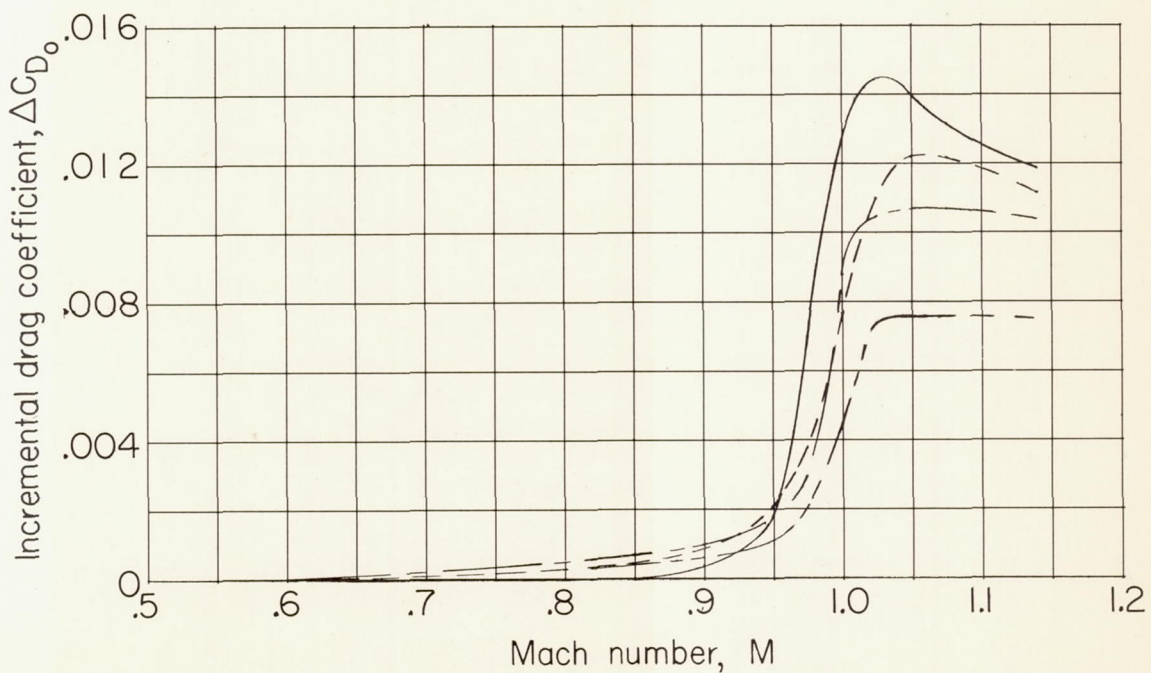
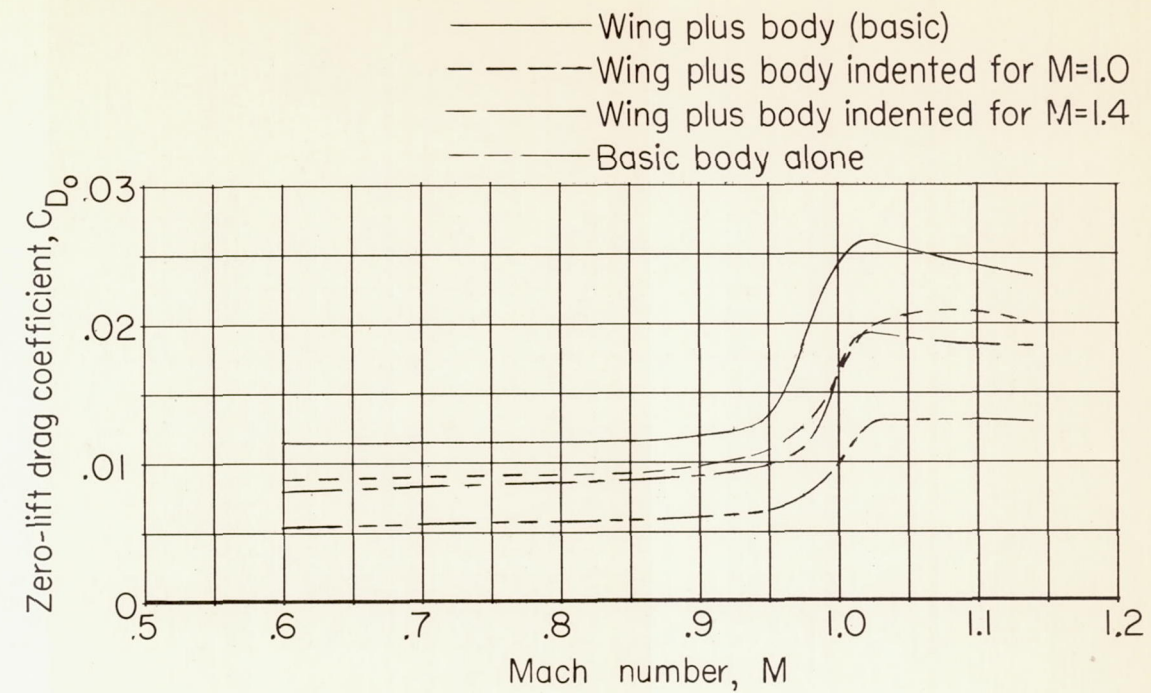
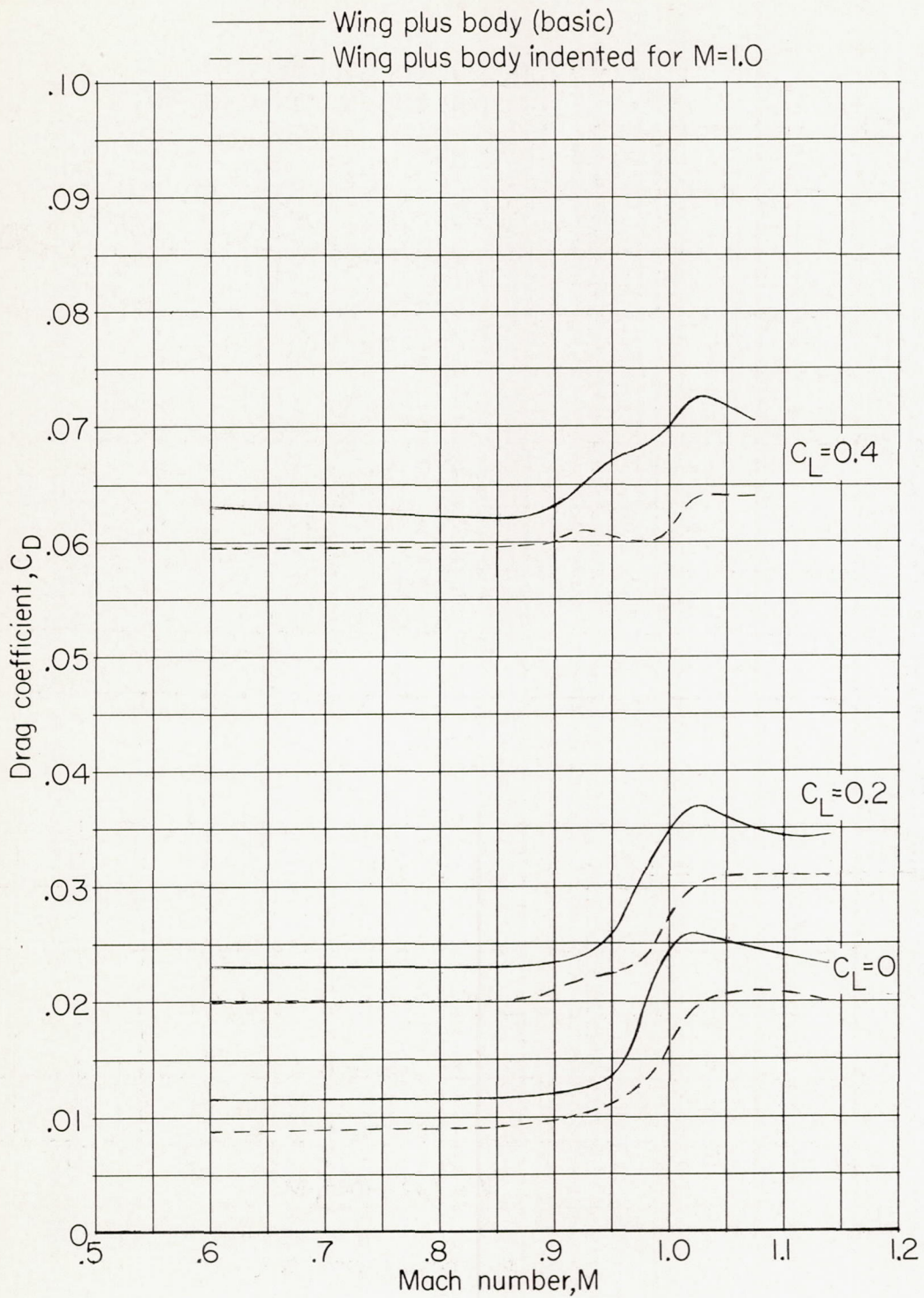
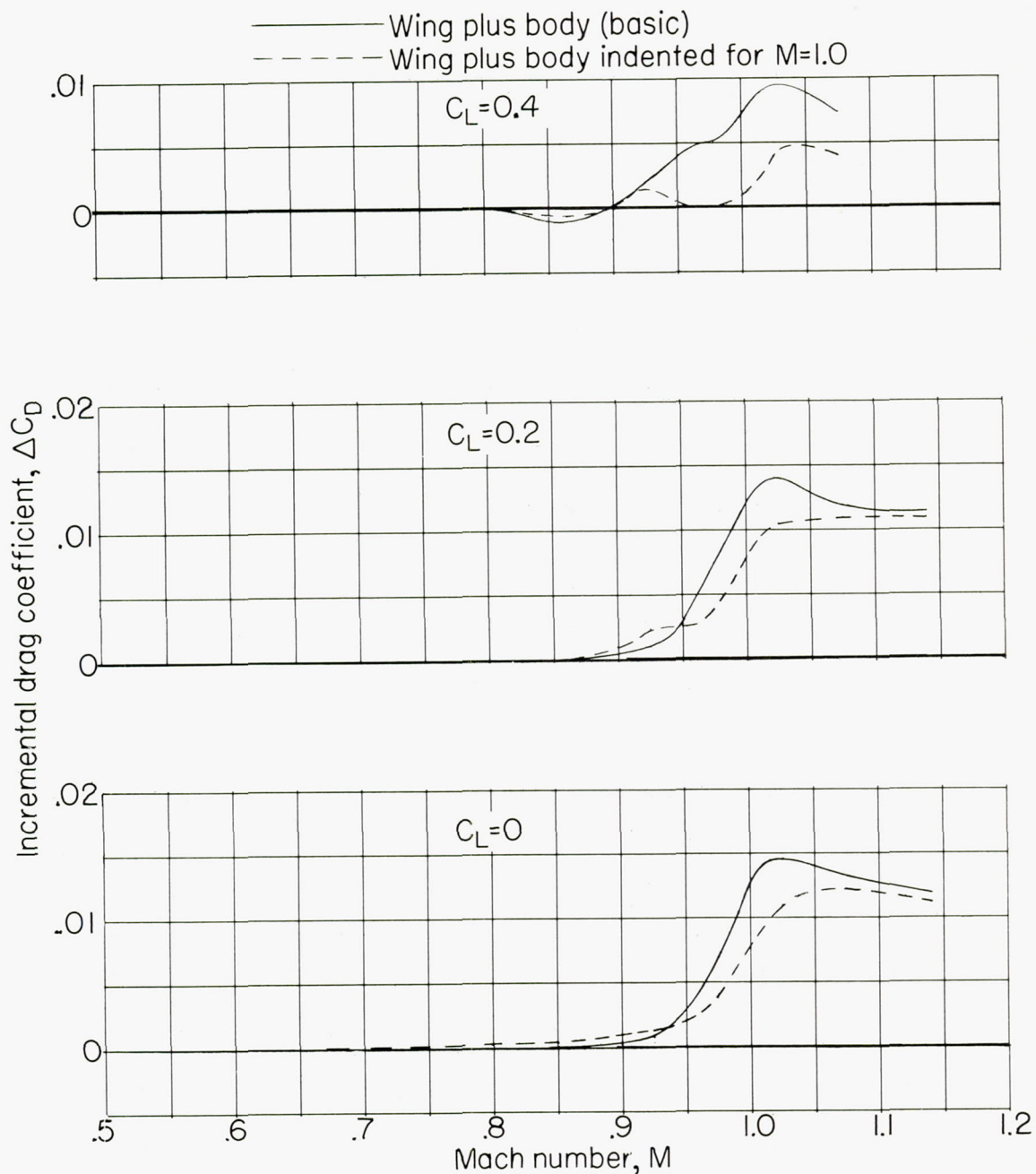


Figure 9.- Effects of transonic and supersonic body indentation on the zero-lift drag and incremental zero-lift drag coefficients.



(a) Total drag.

Figure 10.- Effect of transonic body indentation on drag at lifting conditions.



(b) Incremental drag.

Figure 10.- Concluded.

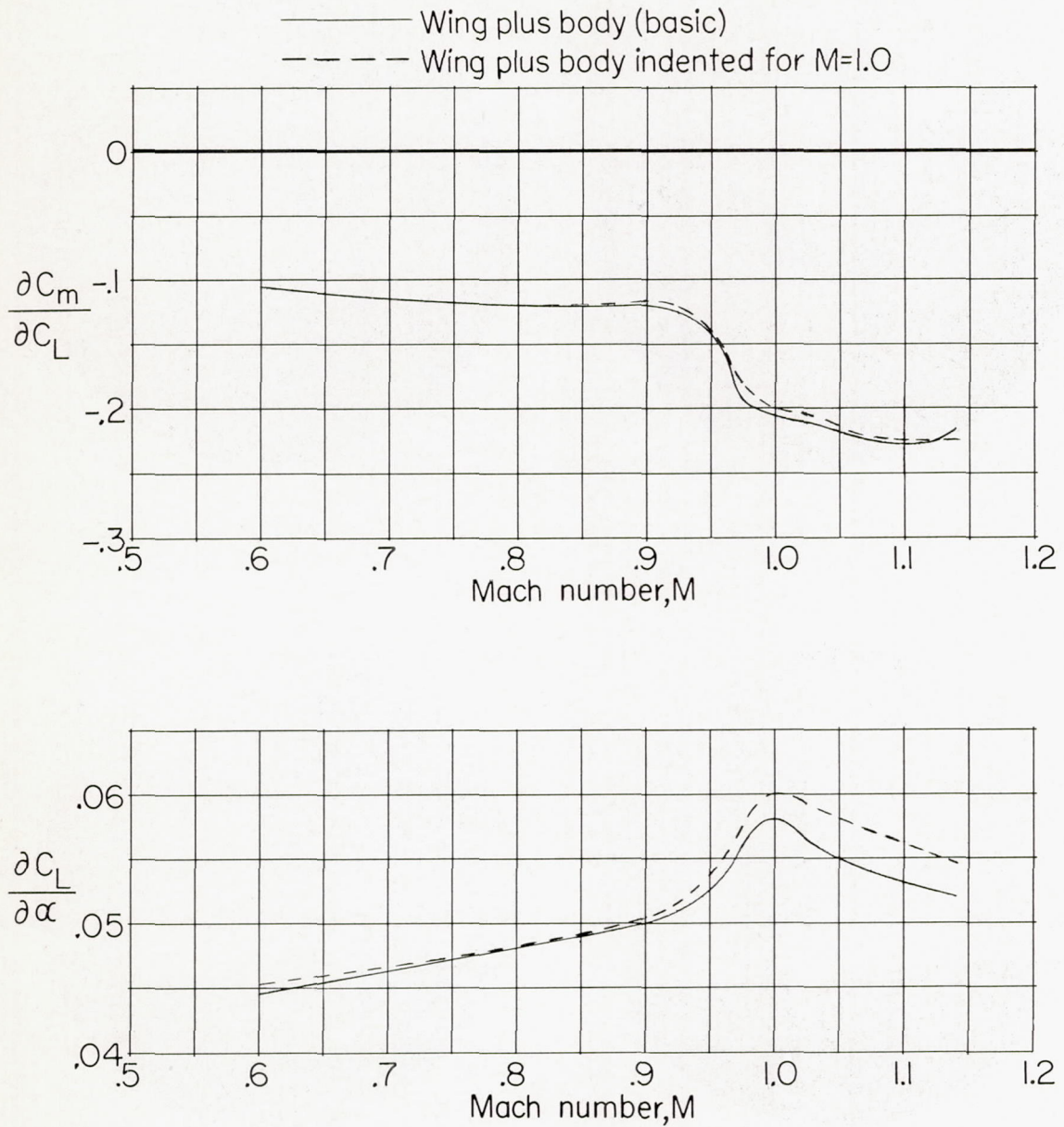
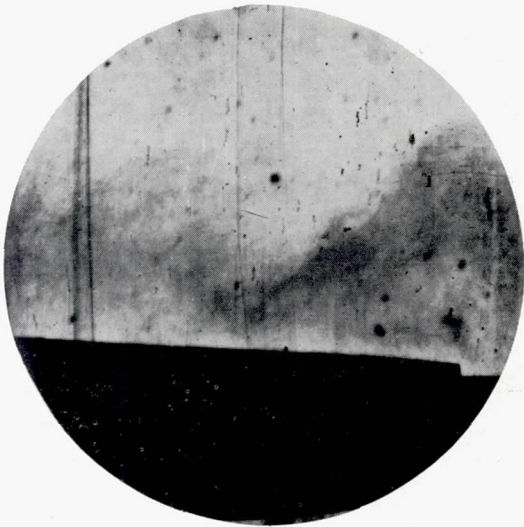
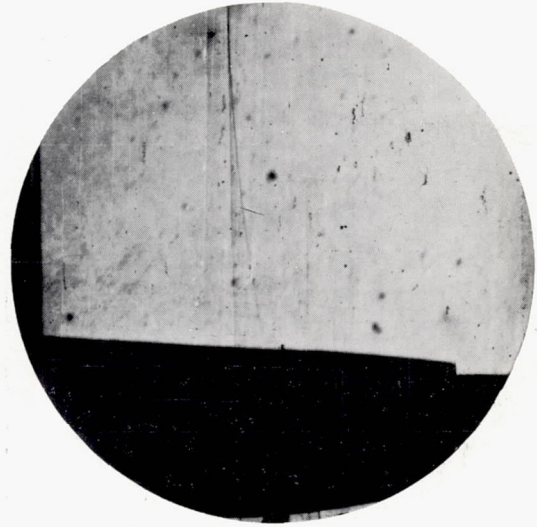


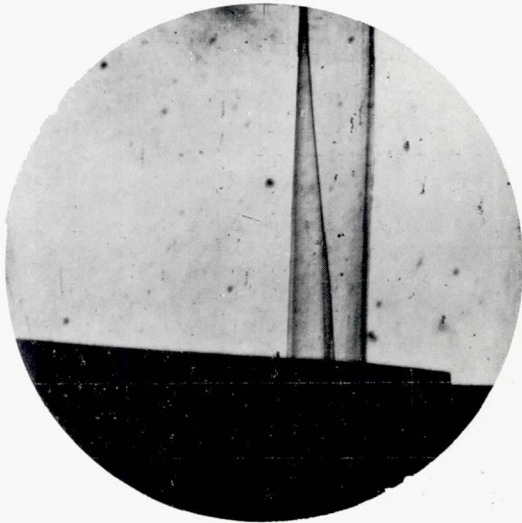
Figure 11.- Effect of transonic body indentation on the average lift-curve slope and static-longitudinal-stability parameter.



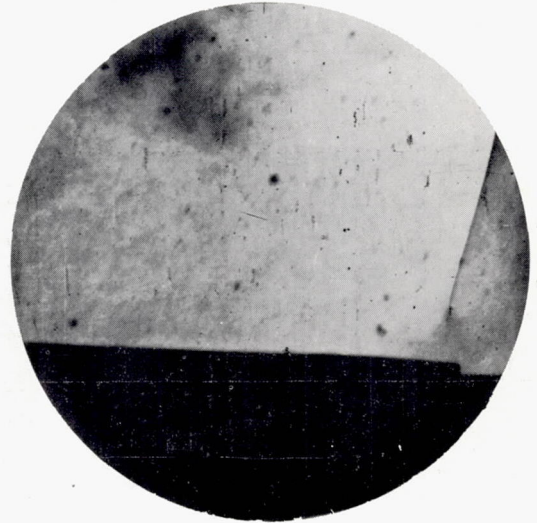
M=0.95



M=0.975



M=1.00

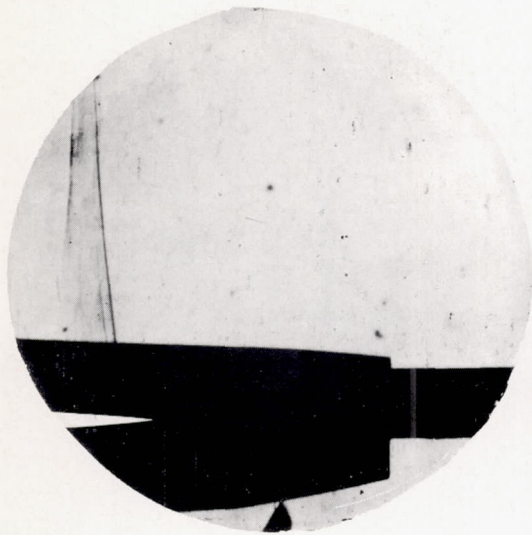


M=1.025

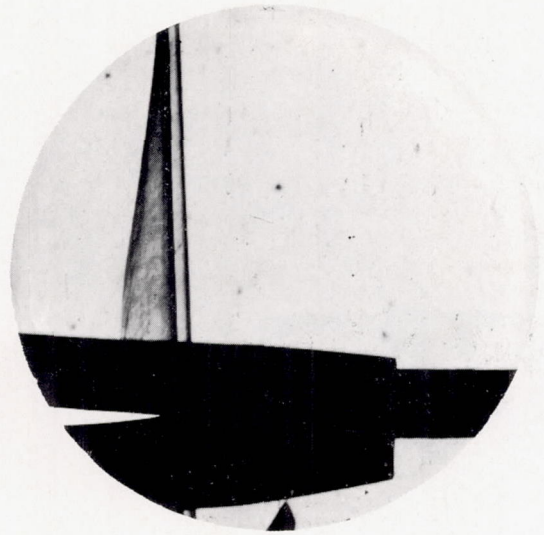
(a) Basic body alone.

L-86465

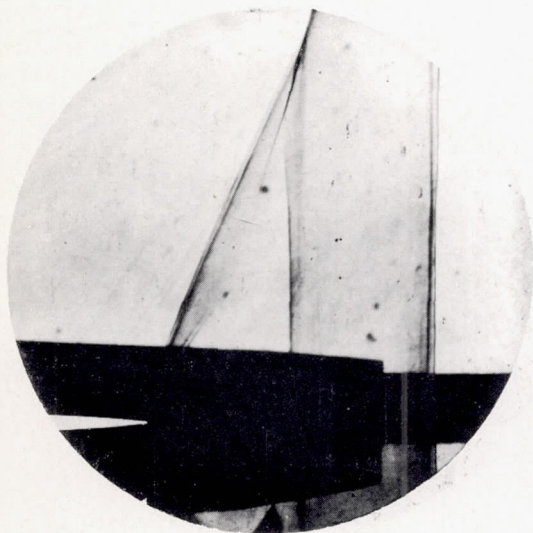
Figure 12.- Schlieren photographs of the configurations tested from Mach numbers of 0.95 to 1.025 at an angle of attack of 0° .



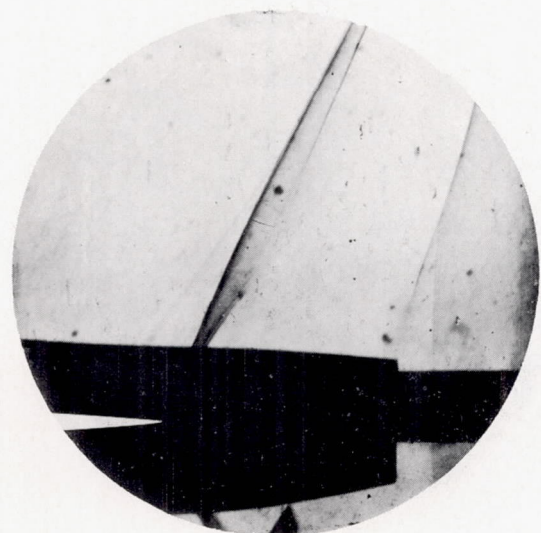
M=0.95



M=0.975



M=1.00

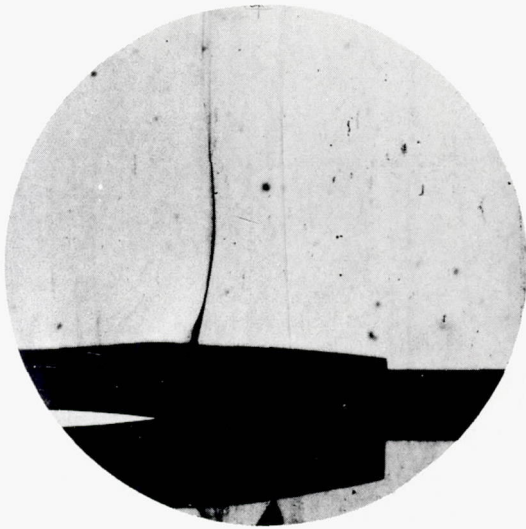
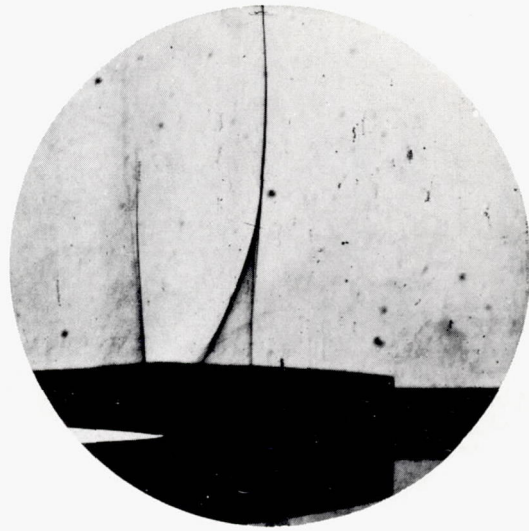
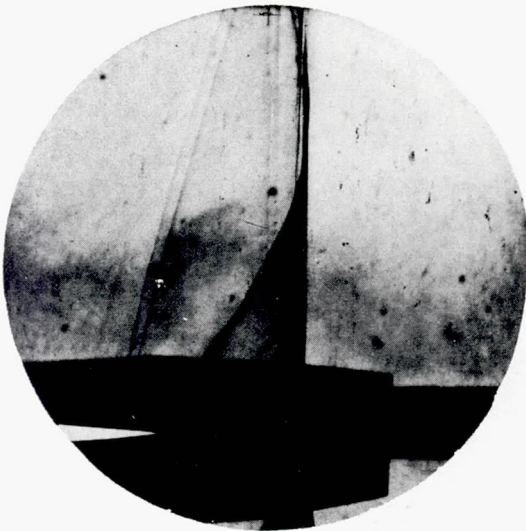
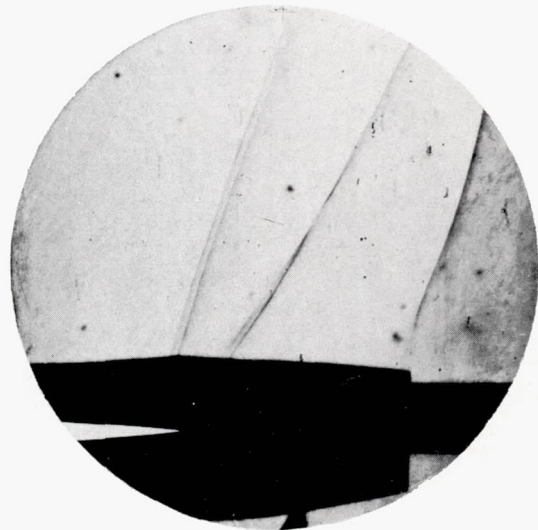


M=1.025

(b) Wing plus body (basic).

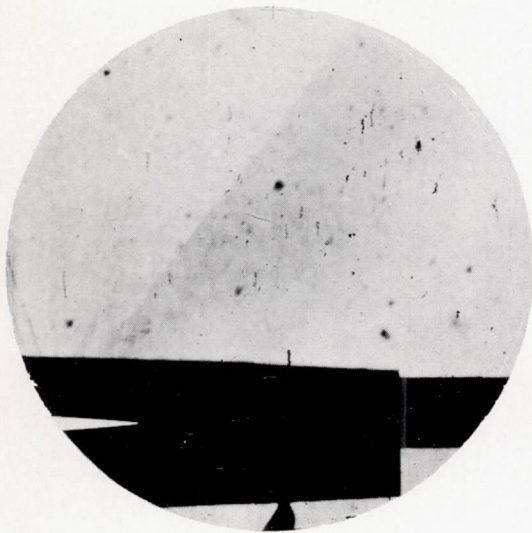
L-86466

Figure 12.- Continued.

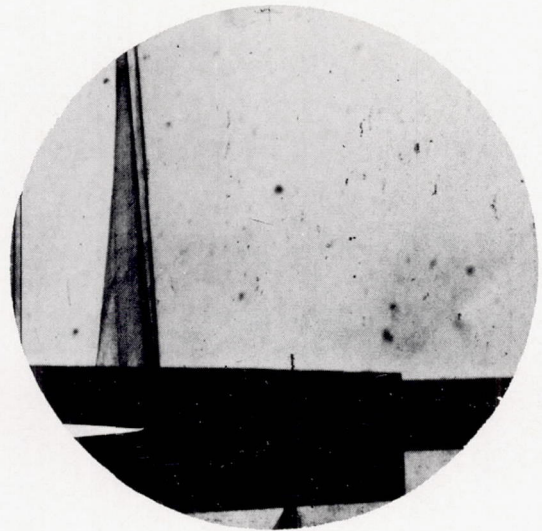
 $M=0.95$  $M=0.975$  $M=1.00$  $M=1.025$

(c) Wing plus body indented for $M = 1.0$. L-86467

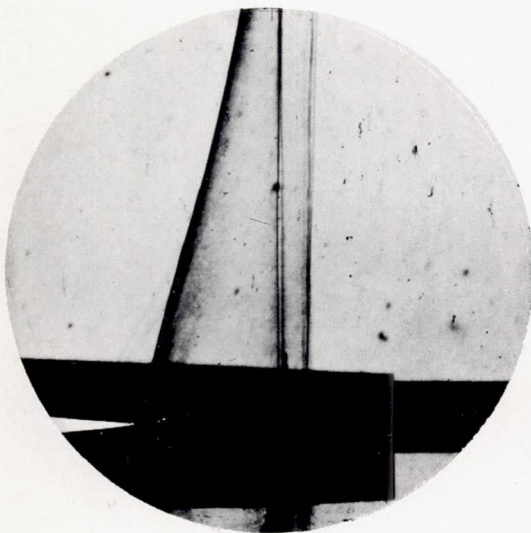
Figure 12.- Continued.



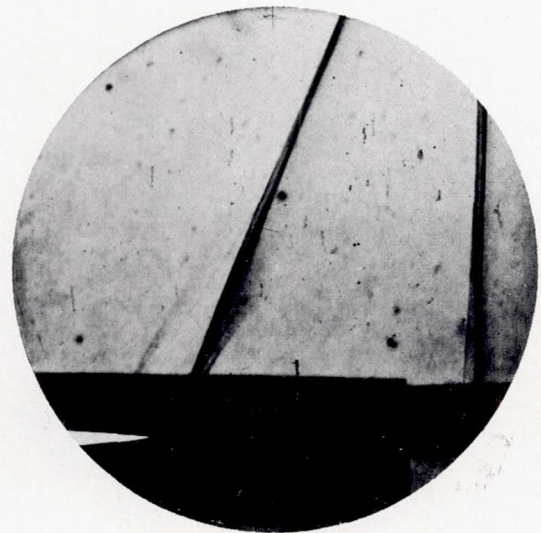
M=0.95



M=0.975



M=1.00

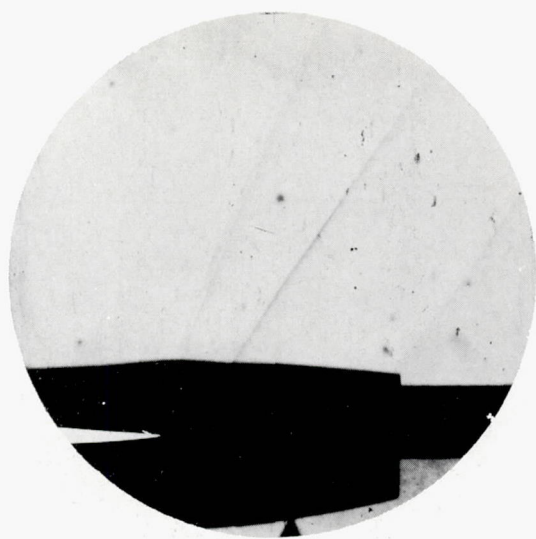


M=1.025

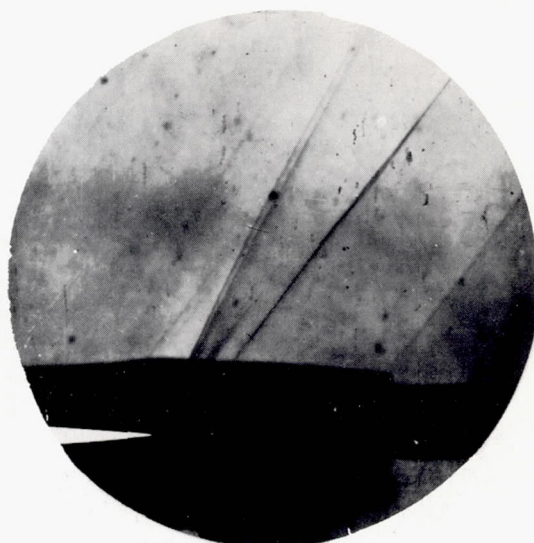
(d) Wing plus body indented for $M = 1.4$.

L-86468

Figure 12.- Concluded.

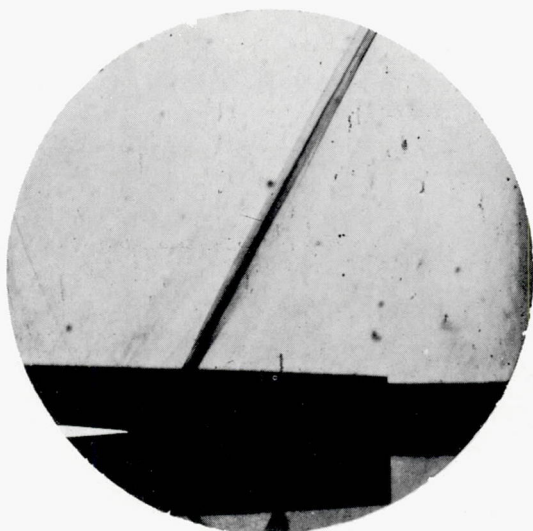


M=1.075

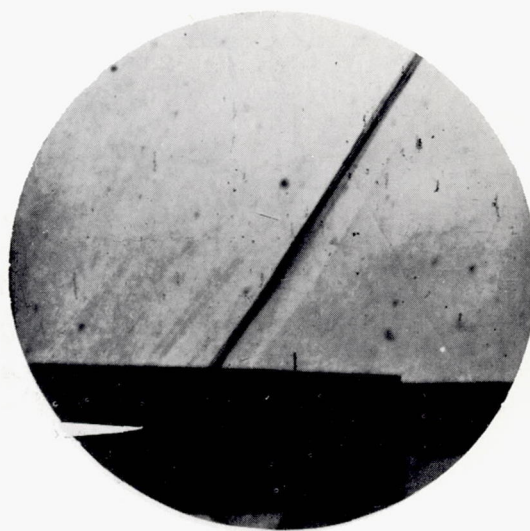


M=1.14

Wing plus body indented for M=1.0



M=1.075



M=1.14

Wing plus body indented for M=1.4

L-86469

Figure 13.- Comparison of shock formation between the wing plus body indented for $M = 1.0$ and wing plus body indented for $M = 1.4$ at Mach numbers of 1.075 and 1.14 at an angle of attack of 0° .

CONFIDENTIAL

CONFIDENTIAL